J. Materials, Conc. Struct., Pavements, JSCE, No. 557/V-34, 159-172, 1997 February

STRESS TRANSFER ACROSS INTERFACES IN REINFORCED CONCRETE DUE TO AGGREGATE INTERLOCK AND DOWEL ACTION

Koichi MAEKAWA[1] and Juneid QURESHI[2]

[1] Member of JSCE, Dr. of Eng., Professor, Dept. of Civil Eng., the University of Tokyo (Hongo 7-3-1, Bunkyo-ku, Tokyo 113, Japan)

[2] Dr. of Eng., Assistant Prof., Dept. of Civil Eng., NED University of Engineering & Technology, Karachi, Pakistan

This paper presents a unified model for RC interface stress transfer, subjected to in-plane shear force, in which the aggregate interlock phenomena and the dowel action are treated together by combination of the newly proposed generic embedded bar model and a physical model for aggregate interlock. The systematic verification through experimental works is conducted for clarifying the versatility of the model proposed.

Key Words *: stress transfer, interlock, dowel action, constitutive Law*

1. INTRODUCTION

For rational analysis of reinforced concrete interfaces, mechanical behaviors of interacting components across the interfaces should be properly conceptualized. Knowledge and modeling related to shear forces in cracked concrete are still not fully understood, because of the fact that shear loading leads to complicated physical mechanisms, such as multi-axial stress conditions, interlocking of cracks, dowel action and reduced bond resistance of embedded bars. It is therefore required to study internal mechanisms of stress transfer and dowel action across RC interfaces in general, whether stress induced or pre-formed.

Two principle modes of shear forces to be transmitted across a crack are either through the interaction between rough surfaces of the crack and through reinforcement crossing the crack. If the reinforcement is normal to the plane of cracking, dowel action will contribute to the overall shear transfer. The tensile stiffness of the reinforcement normal to the crack plane will also influence the shear stiffness of interfaces, since steel bars confine crack widening provoked by overriding of protruding aggregate particles and the confinement brought by reinforcement primarily affects the interlock shear transfer. At the same time the shear displacement at the crack produces localized flexure in reinforcement inside concrete, giving rise to combined flexural and shear stresses, as detailed in previous study [15),16)].

It is clear that both aggregate interlock and dowel action are mobilized by the same system of general forces that are existing at the crack plane and are strictly related to the same crack pattern. Independent formulation for each mechanism and mere superposition, to predict interface stress transfer stiffness and capacity, is not the true representation of the actual interface behavior[7),15)], because of the variable restraint stiffness provided by the reinforcement crossing the crack and the nonlinear interaction between these two shear transfer mechanisms[1),2)].

It is the purpose of this study to propose a unified model for RC interface stress transfer, subjected to in-plane shear force, in which the aggregate interlock phenomena and the dowel action are treated together by combination of the newly proposed generic embedded bar model and a physical model for aggregate interlock.

2. RC INTERFACE SHEAR TRANSFER MECHANISM

Let **Fig.1** show the schematic concrete interface crossed by a reinforcing bar and subjected to shear force V, due to which a relative shear displacement, δ, results. Overriding brought about by crack

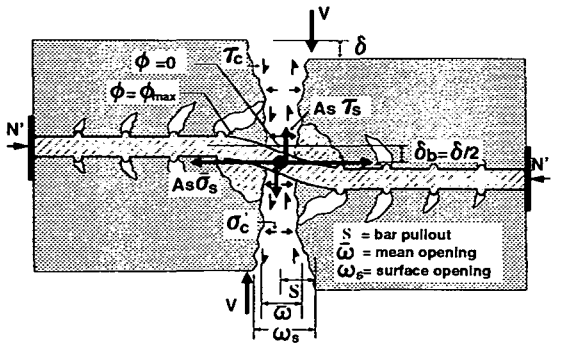

Fig.1 Deformational and mechanical characteristics of a RC interface.

roughness produces dilatancy, i.e., increase in the mean crack width denoted by $\bar{\omega}$. To this dilatancy the reinforcing bar responds by a pullout force $A\bar{\sigma}_s$, due to pullout slip of the bar at the crack, denoted by S. This tension is equilibrated with the compressive force $A_c\sigma'_c$ acting on the concrete. Here, A_s and A_c are cross-sectional areas of steel bar and concrete shear plane. It is mainly due to this compressive force that shear resistance, τ_c, is developed at the interface between concrete asperities.

Along with the concrete contribution to the shear resistance, the reinforcing bar also counteracts the shear displacement of the interface, and this counteraction mechanism is termed as dowel action denoted by $A_s\tau_s$. The shear displacement also introduces curvature in the bar inside the concrete over a certain zone, with a maximum curvature, ϕ_{max}, at some location within this zone[15),16)]. Within this curvature influencing zone, the axial reinforcement stress across its section is no longer only a function of the axial strain but also that of the magnitude of curvature at that location, $\phi(x)$. These parameters as shown in **Fig.1** define the deformational and mechanical characteristics of a RC interface.

In order to compute the coupled shear transfer along an interface and the pullout of reinforcement from embedded concrete, the equilibrium of stresses at a crack are considered as,

$$\sigma'_c = N' / A_c + p\,\bar{\sigma}_s \qquad (1)$$

where, p is the reinforcement ratio and N' is externally applied force defined positive in compression.

By combining the models, formulated and verified separately, for plain concrete stress transfer[3),12)] and bar stress due to axial pullout and transverse displacement [15)], the equilibrium equation (1) can be solved. The constitutive laws which relate these stresses to the displacement state of the interface are of the following.

$$\sigma'_c = \sigma'_c(\delta, \bar{\omega}) \qquad (2)$$

$$\bar{\sigma}_s = \bar{\sigma}_s(S, \delta_b) \qquad (3)$$

where δ_b is the transverse displacement of the bar. The dependency of $\bar{\sigma}_s$ on both axial pullout and transverse displacement represents the major concept behind the two dimensional idealization of an embedded bar and which led to the formulation of the generic embedded bar model, as detailed in the reference (15).

The compatibility between the normal and transverse displacements of the concrete and for the reinforcing bar is expressed as,

$$\delta = 2\,\delta_b \quad ; \quad \bar{\omega} = c\,(2\,S) \qquad (4)$$

where, factor c indicates the variation in crack width from the surface of the bar to the concrete surface (see **Fig.1**) and will be discussed later.

Once the displacement paths satisfying the equilibrium normal to the interface are found, the constitutive laws relating the shear stresses of the concrete, τ_c, and the steel, τ_s, parallel to the interface, present the total shear transferred, τ_t , by superposition.

$$\tau_t = \tau_c + p \cdot \tau_s \qquad (5)$$

$$\tau_c = \tau_c(\delta, \bar{\omega}) \qquad (6)$$

$$\tau_s = \tau_s(S, \delta_b) \qquad (7)$$

Here, the aggregate interlock model used in Eq.(2) and Eq.(6) is the proposed universal stress transfer model[11),12),13)]. This model is attractive for its comprehensiveness and versatility to deal with the complex phenomenon of stress transfer across cracks in concrete. The model is based on the assumption that a crack surface consists of a set of differently oriented contact plane[8)]. For the constitutive model of reinforcing bars used in Eq.(3) and Eq.(7), the authors adopted the enhanced modeling of coupled pullout and dowel action of steel in consideration of localized plasticity of reinforcement close to the cracked interface [15)].

3. LOCALIZED DETERIORATION AND NON-UNIFORM DILATANCY

The concrete stress transfer model was derived from the plain concrete behavior, but it has been clearly manifested[7)] that the simple superposition of this model with a embedded bar model does not give satisfactory results. One primary reason was the deficiencies inherent in the one dimensional idealization of the bar model when applied to the problem of crack shear, and this was addressed in

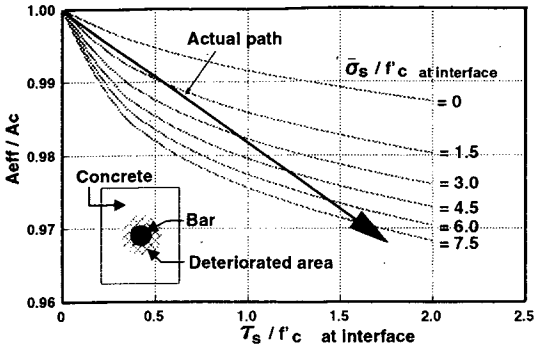

Fig.2 Variation of effective concrete area for stress transfer with influencing parameters.

the reference (15). Also, the stress transfer behavior in reinforced concrete differs from that of plain concrete. This is due to the steel pullout and transverse displacement at RC interfaces, which interacts with the concrete stress transfer performance.

One such interaction is the relaxation of the bearing properties of the supporting concrete along the bar axis, which manifests itself in the axial effectiveness of the reinforcing bar. This behavior was addressed in the reference (16). Another interaction effect is the local damage of concrete around a steel bar. Also, concrete crack dilatancy in the presence of embedded bars differs from that in plane concrete, due to the local bond between the concrete and bar [14].

It is clear that the plain concrete stress transfer model needs the incorporation of some additional concepts to enhance its applicability to RC interfaces. These concepts are related to the deterioration due to interactive stresses imparted from the reinforcement to localized areas of surrounding concrete on the interface plane, and the non-uniform crack opening or dilatancy across the shear plane due to localized concrete deformation near reinforcement.

(1) Localized damage zones surrounding embedded bar at concrete interface

It is known that the presence of numerous micro-cracks in the concrete surrounding each bar produces localized damage zones[14]. These cracks can be attributed to the radial bond cracks around the bar periphery and cracks due to increasing bearing stresses supporting the transverse movement of the bar. Also, there is no local shear slip of the crack plane at the intersecting point of the steel and crack plane, which also manifests itself in the loss of effective shear plane for concrete stress transfer.

Here, it is assumed that a certain area exists surrounding the bar where the contact stress-deformation relation formulated for plain concrete does not hold valid and the overall stress transfer phenomena is reduced. To take this into account, a localized damage area, A_{det}, concept is introduced, through which the reduction of stress transfer due to a locally deteriorated area is computed. The damage area is thought to be a function of the mean axial and shear stress of the bar at the interface, and expressed in terms of an interface damage index as

$$DI' = \log\left[1 + 4\left(1 + \frac{\bar{\sigma}_s}{f'_c}\right)\cdot\frac{\tau_s}{f'_c}\right] + 1$$
$$A_{\det} = \frac{\pi}{4}\cdot(DI'\cdot D)^2 \qquad (8)$$

where, f_c' is uniaxial compressive strength of concrete and D is a diameter of a bar concerned.

The shape of the functional form represents the implicit assumption that the rate of damage in the concrete, treated as a macroscopic internal state variable, increases at a decreasing rate with the increase of the influencing parameters. The effective concrete area, A_{eff}, substantially contributing to stress transfer is gradually reduced as the deteriorated area around the bar increases, as shown in **Fig.2**.

$$A_{eff} = A_c - \sum_{i=1}^{n} A_{\det} \qquad (9)$$

where n is the total number of bars crossing the interface.

It is emphasized here that the above model is the concrete deterioration model around the shear plane.

(2) Variable crack width along RC interface

In the case of a RC interface crossed by deformed bar(s), the width of the crack at the bar surface does not remain uniform away from the surface[14]. From the test data available it is seen that in general the surface crack widths, ω_s, are nearly similar to twice the pullout slip S, defined from the free end of the bar, as shown in **Fig.3**. In the present model, in order to predict not only the shear transfer but also the deformational relationship between δ and ω_s, an idealized crack surface variation is assumed by introducing compatibility relation as

$$\omega_s = 2S \quad :\bar{\omega} = c(\omega_s) \quad (c = 1/1.3) \qquad (10)$$

The value of c represents the internal crack gap geometry, and if it would be of linear profile, c=1/2. For prediction of experimental results, as will be shown in following sections, the value of c is

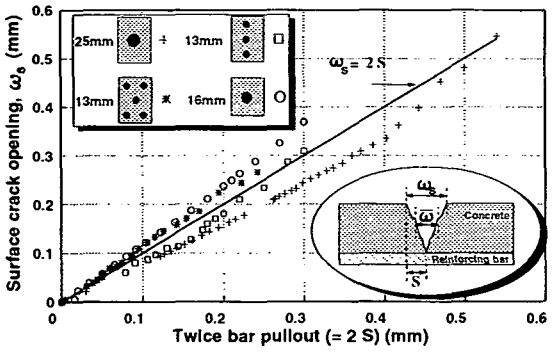

Fig.3 Relation between bar pullout and surface crack opening from test results.

tentatively held constant at 1/1.3. More experimental results are required to formulate an generalized expression for c, which should be rationally formulated dependent on concrete cover, bar size, bar interspacing, etc.

4. ULTIMATE SHEAR CAPACITY OF RC INTERFACES

In order to obtain the ultimate shear capacity of a RC interface, it is necessary to define the failure criterion which will govern the ultimate capacity. For usual material properties for deformed bars, the localized yielding and consequent reduction of confining axial stiffness and strength of the bar is the predominant failure mode determinator as verified through test results discussed in the reference (16).

But, other failure conditions may limit the maximum shear stress across a RC interface such as splitting of concrete cover and excessive plastification and fracture of concrete contacting units across the interface. This section describes the determinators of ultimate shear capacity.

(1) Loss of confinement imparted by embedded bar

The primary failure criterion for the interface is due to the loss in confinement given by the embedded reinforcement to the crack plane. This is initiated by the formation of a plastic hinge in the reinforcement due to the combined bending moment, shear and axial forces induced in the reinforcement as a result of the pullout and shear slip to which it is subjected at the interface. The ultimate confining axial stress provided by the embedded bar is defined by the limiting criterion, $\lambda(x)$, for interactive stresses produced due to bending moment, $M(x)$, shear force, $V(x)$, and axial force, $P(x)$, on the bar. This is derived on the basis of the limit stress field possible across the bar section with yield strength of f_y under interactive forces as,

$$\lambda(x)=\left[\frac{M(x)}{M_o}+\left(\frac{P(x)}{P_o}\right)^2\right]^2+\left[\frac{V(x)}{V_o}\right]^2=1 \qquad (11)$$

where, M_o ($=f_y D^3/6$), P_o ($=A_s f_y$) and V_o ($=A_s f_y/\sqrt{3}$) are the ultimate values of these parameters under non interactive force conditions. Under any combination of the interacting forces, $\lambda(x)$ equaling unity implies the ultimate bar axial capacity. Details regarding the applicability and experimental verification of such an interaction criteria is given in the reference (15).

Once the plastic hinge forms, the bar is incapable of taking any further increase in bending moment, and any additional transverse displacement cannot be balanced by an increase in bar curvature. This leads to a collapse mechanism initiating rotation of the bar from the plastic hinge location and a loss of the confining force necessary to mobilize the interface friction. Although at this point shear resistance by kinking of the bar might become significant, but the overall shear transfer would reduce. Localized strain gage readings from experiments conducted verify that this is the usual mode of failure for a RC interface.

(2) Splitting of concrete cover

There exist two mechanisms which are activated when an embedded reinforcement pushes against the supporting concrete due to induced displacement transverse to the reinforcement axis. One is the 'strong' mechanism when the bar pushes against the concrete core. The other is the 'weak' mechanism initiated by the bar pushing against the concrete cover.

In the latter case the transverse force in the bar is idealized to be balanced by tensile stress developing in concrete cover. If concrete strength is low, bar diameter is high and sufficient cover is not provided for the reinforcement, the shear capacity could be dictated by the 'weak' mechanism and failure is governed by consideration other than localized plastic hinge formation in the reinforcement, as described in the previous section. Under such cases failure would be initiated due to side splitting along a certain length of the reinforcement.

For considering side splitting stresses, the compressive bearing stresses, $f_b(x)$, induced below the bar have to be equilibrated by resultant tensile stresses around the bar (see **Fig.4**). The failure condition can be determined through this

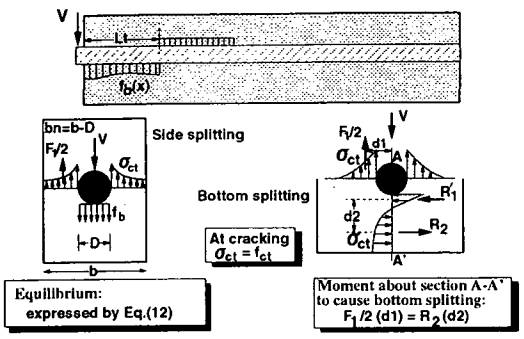

Fig.4 Conceptual modeling for side and bottom splitting failure conditions in RC interfaces with insufficient cover where; R_1' & R_2: comp. & tensile resultant forces, f_{ct}: tensile strength.

equilibrium condition, and by assuming a distribution profile for the tensile stresses, σ_{ct}, along the width of the specimen. If the distance from the interface to the point where the equilibrating tensile stresses are present in the concrete is denoted by L_t, we have the equilibrium for the total tensile force given by,

$$D \int_{L_t} f_b(x)\, dx = L_t \int_{b_n} \sigma_{ct}(b)\, db = F_1 \qquad (12)$$

where, b_n is the effective width supporting tensile stresses, and D is the bar diameter. The relevant stress fields are shown in **Fig.4**. It is then postulated that a horizontal crack opens up along the axis of the bar as the tensile stresses in the concrete along the sectional width progressively attains its tensile strength, f_{ct}.

In the case of very small bottom cover to the reinforcement, as compared to the side cover, a bottom splitting failure can be initiated before side splitting. A similar expression can be derived for consideration of bottom splitting failure, by assuming a simplified self equilibrating stress distribution below the bar along a plane normal to the bar axis. By taking moments about a plane passing through the bar axis, the critical bearing stress profile to produce tensile cracking below the bar can be computed, as shown in **Fig.4**.

Within this study, only the 'strong' mechanism of embedded bar behavior has been concentrated on, and test results selected were those in which splitting failures were not observed. However the easily extensible generic applicability of the proposed model to cover other failure conditions, by idealizing the relevant tensile stress profiles in the concrete, is evident from the above discussion.

(3) Miscellaneous failure conditions

Although the above two criteria are the most commonly occurring failure determinants in usual RC interfaces, several other conditions can be conceptually considered which might control interface shear capacity. In the case of very smooth interfaces with negligible aggregate interlock, the pullout of the reinforcement would be very small and as such capacity would predominantly be decided by the dowel strength of the embedded bars. This failure mode is coherently covered by the present model.

In the case of reinforcement having very high yield capacity and concrete of low strength, it might be theoretically possible for the interface capacity to be determined by the 'failure' of the concrete at the interface, due to excessively large crack opening and shear displacement through which shear cannot be further transferred, because of the plastification of the contact units on the concrete surface. This can also be treated by the present model due to the inherent physical macroscopic models of elasto-plastic contact stresses, anisotropic plasticity and contact fracturing incorporated in the aggregate interlock model [12].

5. COMPUTATION OF IDEALIZED MODELS ON SHEAR TRANSFER

The proposed model incorporates both the embedded bar model and the concrete aggregate interlock model to predict the stress transfer behavior of RC interfaces. Here, the effective area of concrete was used to compute the concrete shear force from the shear transfer stress and computation was terminated when the above stated failure conditions were satisfied. A numerical algorithm is utilized for the computational scheme[3].

For checking sensitivity of the newly introduced concepts other than previously proposed models, computations were carried out by switching off the effect of various concepts, collectively or individually. The sensitivity of the concepts for deteriorated area around the bar at the interface and that for the non-uniform dilatancy of RC interface are shown in **Fig.5**.

The use of the deteriorated area increases the shear slip and reduces shear stiffness by a small amount, whereas the introduction of non-uniform dilatancy primarily increases the surface opening observed at the interface. The use of only one of these two ideas either reduces the surface opening and increases shear displacement, or reduces the shear displacement and increases shear stiffness. Both concepts together creates the correct balance for shear stiffness, capacity, shear displacement and surface opening.

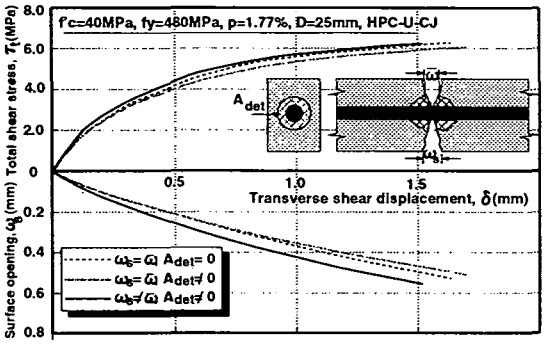

Fig.5 Sensitivity of concepts introduced in aggregate interlock model : HPC-U-CJ = high performance concrete, unprocessed construction joint.

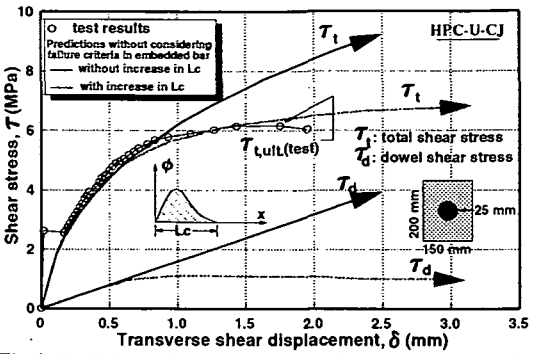

Fig.6 Predictions of shear stress-shear displacement relation for test data of a typical specimen (Specimen 4 in ref. 16) without consideration of failure criteria in bar.

However, it should be noted that the sensitivity is not large and even without these concepts satisfactory predictions would be obtained in many cases, specially for the shear capacity. The use of these two philosophies which are physically rational, but are not directly verified from test results, is to improve the displacement predictions associated with the capacity to some extent, but no extraordinary changes are attempted through such concepts.

The sensitivity of the failure criterion for the embedded bar, which was verified with the bar pull-out stiffness and capacity data in the reference (15), is again checked here with the shear transfer test data[16] of a typical specimen as shown in **Fig.6**, where analysis with and without the increase in the curvature influencing zone, in which bending action develops (denoted by L_c) are illustrated. From the analysis it can be seen that if the interaction failure condition in the bar is not considered, the analytical results would over-predict test data. Consideration of the increase in curvature influencing zone[15] reduces the shear stiffness. If no increase in the zone size is considered then the stiffness degradation is less, due to increase in dowel shear in the absence of any failure criterion for the bar. Therefore, the validity of the use of the interaction equation for determining maximum bar axial confining stress under combined axial, shear and bending forces is once again verified, this time by comparison with the shear transfer results.

6. VERIFICATION OF STRESS TRANSFER MODEL

Although the generic bar model has been independently verified[15], its true applicability will be clear after combining with a concrete aggregate interlock model, because displacement paths at the interface will be dependent on the equilibrium and compatibility requirements at the real interface.

In order to clearly examine the reinforcement behavior under high shear slip to crack opening ratios, some tests were carried out on self-compacting high performance concrete (HPC) construction joints imparting a very smooth surface asperity[16] and these data were herein used for verification. The geometrical feature of joint surface can be accounted for by a modified contact density distribution function which represents a steeper orientation of contact units[3].

(1) Ultimate shear capacity

a) Reinforcement normal to shear plane

The ultimate shear capacity of a RC interface is governed by the maximum confining stress provided by the reinforcement crossing the interface plane. This maximum confining strength is a function of the reinforcement ratio, the concrete compressive strength, f'_c, the geometrical surface roughness of the interface and the reinforcement yield strength, f_y. The first three parameters govern the displacement path at the interface, thereby determining the maximum axial stress possible under combined stresses for a given reinforcement yield strength.

Prediction of ultimate shear capacities by the proposed model for normal concrete (NC), rough cracks (RC), series tests with reinforcement crossing normal to the shear plane, done in previous research works[4),5),10)], is shown in **Fig.7**. These tests were performed on push-off specimens with or without external normal compressive forces. The 'strong' mode bar to concrete interaction, i.e. bar pushing against concrete core as opposed to concrete cover, was dominant since failure by splitting of cover was not observed in the tests due to sufficient cover or concrete strength. The failure then was dictated by the loss of confining stress to the generated cracks. The low coefficient of variation observed between

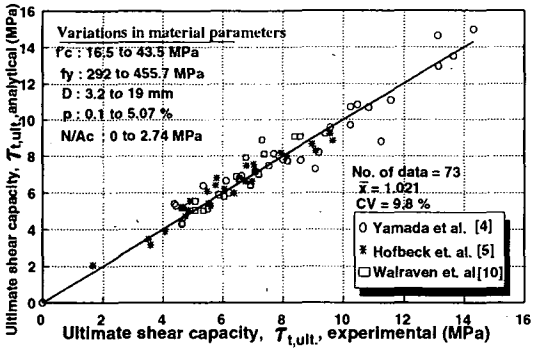

Fig.7 Prediction of ultimate shear capacity of normal concrete rough crack test data.[4),5),10)]

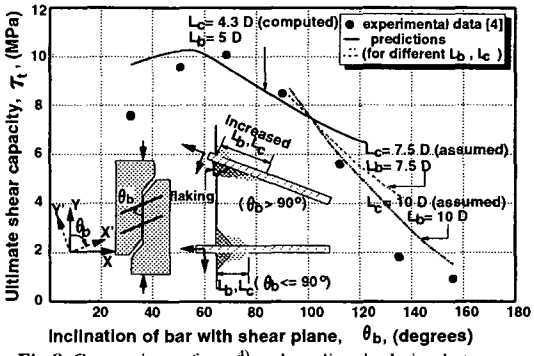

Fig.8 Comparison of test [4)] and predicted relation between shear capacity and bar angle with shear plane.

test and predicted results for the wide range of material parameters selected indicate the accuracy and versatility of the proposed model. In general the accuracy is better than most of the empirical equations given in previous researches for determining shear capacity of RC rough cracks [5),9)].

b) Reinforcement oblique to shear plane

When reinforcing bar axis is oblique to the shear plane, both axial and dowel shear forces in the bar contribute as a part of shear carrying mechanism. Transformation of local displacements and stresses for a coordinate system defined with respect to bar axis to global displacement and stresses for a coordinate system defined with respect to the shear plane, gives the following compatibility and equilibrium relations.

$$S = \frac{\delta \cos\theta_b + \omega_s \sin\theta_b}{2}$$
$$\delta_b = \frac{\delta \sin\theta_b - \omega_s \cos\theta_b}{2} \qquad (13)$$

$$\sigma_c = p \cdot \overline{\sigma}_s \sin\theta_b - p \cdot \tau_s \cos\theta_b \qquad (14)$$

$$\tau_t = \tau_c + p \cdot \tau_s \sin\theta_b + p \cdot \overline{\sigma}_s \cos\theta_b \qquad (15)$$

where, θ_b is the angle between the shear plane and the bar axis, defined according to the sign convention shown in **Fig.8**.

The formulation of the curvature influencing zone (L_c) and the bond deterioration zone (L_b) detailed in the reference 15 were mainly verified for bars at right angles to the shear plane. It is clear that if the bar is at an angle greater than 90°, the bearing resistance of the supporting concrete is reduced as the bar pushes against a less confined free surface between the bar and the interface, inducing concrete flaking at large bar angles. Then, L_c would be increased for such cases, mutually increasing the bond deterioration zone L_b.

Ultimate shear capacity computed for test data from literature[4)] for different bar angles with the rough crack shear planes, indicates that for angles greater than 90°, L_c needs to be increased to predict test results, which is rationally justified from the mechanics of the bar pushing not against the concrete core, but against less confined free surface of the supporting concrete. The predictions are shown in **Fig.8**, by considering different zone sizes for curvature and bond deterioration. Satisfactory correlation can be obtained, considering the small number of such data available, through which the applicability range of the proposed RC stress transfer model is understood and extended.

(2) Verification of stress displacement relation

Predictions for the complete shear stress and associated interface displacement, from load initiation to ultimate shear capacity, were also attempted for test results conducted for this study and some typical ones from literature[16)]. Equilibrium and compatibility conditions at the interface require that only through the accurate analytical modeling of the concrete and embedded bar nonlinear behavior, all the predicted parameters, i.e. shear stress transferred, τ_c, the interface shear displacement and dilatancy, δ and ω_s respectively, and the confining bar stress, $\sigma_{s,ult}$, at the ultimate shear capacity, can be predicted.

Test results indicate that the shear stiffness of the stress transfer behavior is highly nonlinear, the source of which must be the concrete plasticity and the localized nonlinearity in the steel which effects the steel stress and pullout relation at the interface. The nonlinear stiffness, ultimate shear capacity and the confining steel stress can be satisfactorily predicted by the proposed model as shown in **Fig.9**, for some typical specimens tested[16)], which included processed (P), and unprocessed (U), high performance concrete (HPC), construction joints (CJ). Similar predictions for normal concrete (NC) and rough cracks (R.Cr) from typical results available in literature[4),7),8),9)] are shown in **Fig.10**.

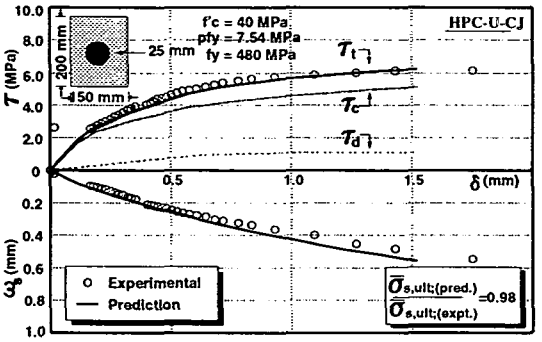

(a): Interface shear stress vs. associated displacement.
(Specimen 4)

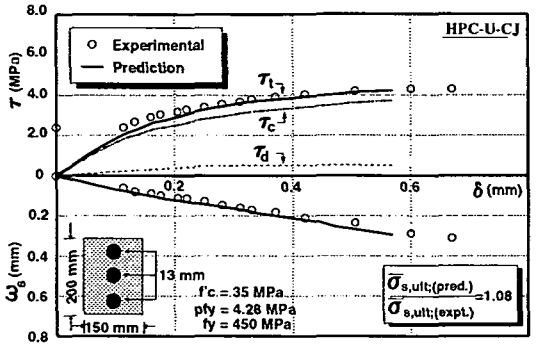

(b): Interface shear stress vs. associated displacement.
(Specimen 5)

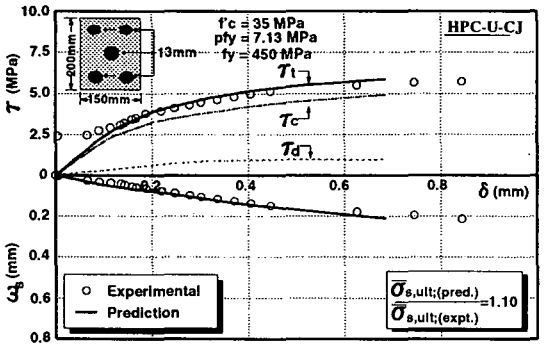

(c): Interface shear stress vs. associated displacement.
(Specimen 6)

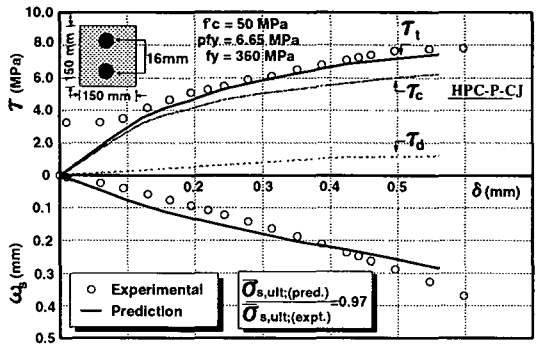

(d): Interface shear stress vs. associated displacement.
(Specimen 7)

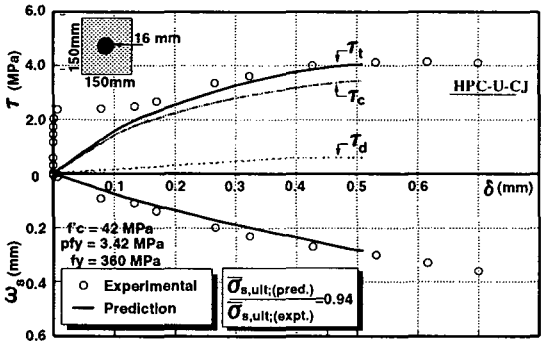

(e): Interface shear stress vs. associated displacement.
(Specimen 9)

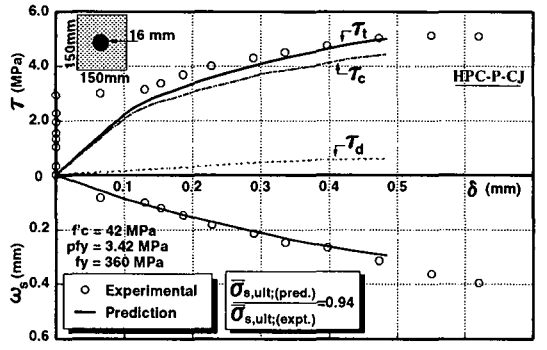

(f): Interface shear stress vs. Associated displacement.
(Specimen 10)

Fig.9 Comparison of predicted and experimental results of shear stress-associated displacement relation at interface, along with maximum confining mean axial stress of reinforcement at failure, for authors' tests. [16]

The proposed model unifies the concept of shear transfer by aggregate interlock and dowel action and both mechanisms are treated simultaneously. **Fig.9** and **Fig.10** show the total shear stress transferred, τ_t, along with the relative proportions shared by concrete and steel, τ_c and τ_d, respectively. The relative proportions of dowel contribution range from 5% to 25%, depending on the reinforcement ratio, the concrete strength, the bar diameter and the general geometrical roughness of the interface. This is in general agreement with previous test results[7]. The rate of increase of the shear carried by each mechanism decreases with the increase of associated displacement paths, δ and ω_s, because of the plasticity and fracturing of the contact units at the interface[3] and the gradual increase in the zone of curvature in the bar, as explained in the reference[15),16)].

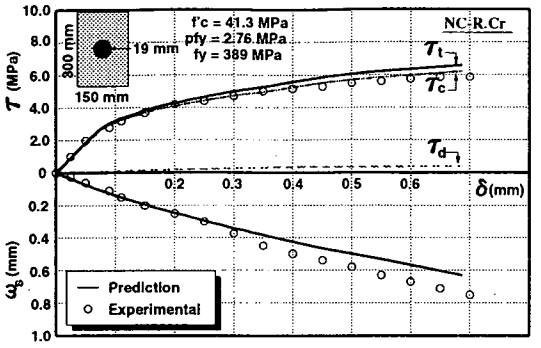

(a): Prediction of results from reference (8).

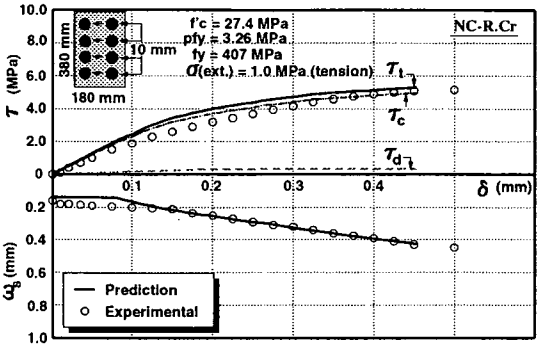

(b): Prediction of results from reference (7).

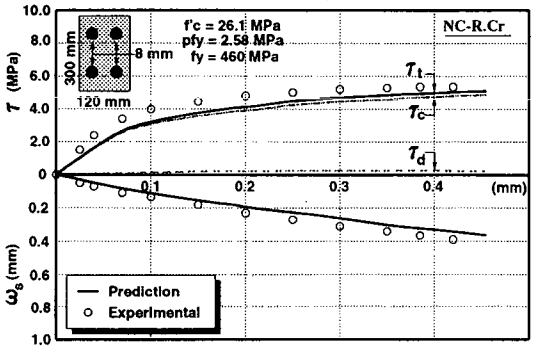

(c): Prediction of results from reference (9).

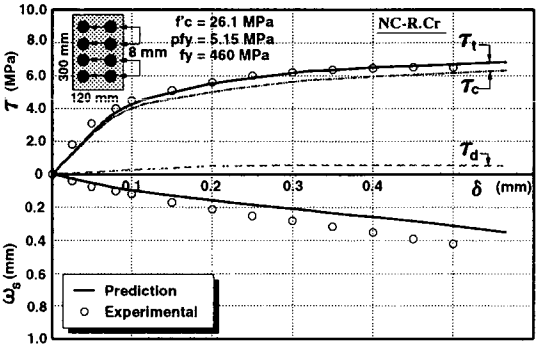

(d): Prediction of results from reference (9).

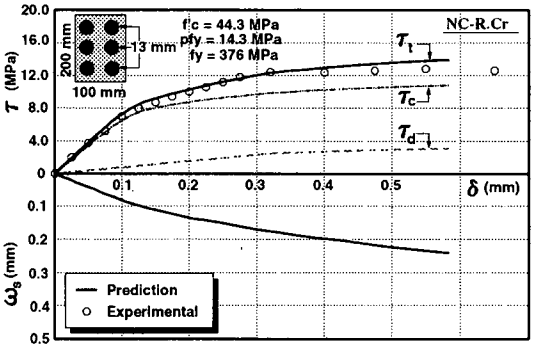

(e): Prediction of results from reference (4).

Fig.10 Comparison of predicted and experimental results of shear stress-associated displacement relation at interface, from the literature.

7. EFFECT OF REINFORCEMENT RATIO ON RC INTERFACE MECHANICAL BEHAVIOR

Since the versatility and accuracy of the proposed RC stress transfer model has been checked, it can be used for the clarification of the mechanical behavior of RC interfaces through numerical simulation. The effect of reinforcement ratio, which is the single most dominant parameter to influence the interface shear capacity is studied for normal concrete rough cracks with common material property parameters. The variation of ultimate shear capacity with increase in uniaxial stress capacity is shown in **Fig.11**.

It is seen that the actual ultimate confining stress to the interface, expressed as $p\overline{\sigma}_{s,ult}$, is much less than the pure axial capacity of pf_y, because of the combined

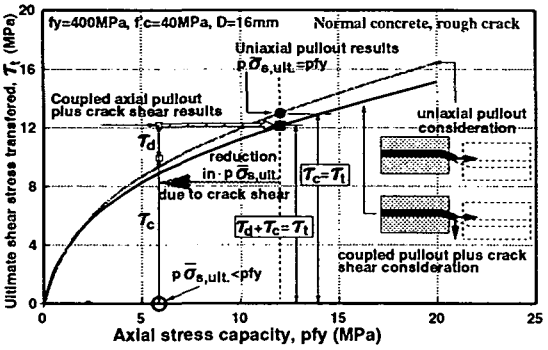

Fig.11 Simulation of ultimate shear stress versus maximum uniaxial stress capacity. (uniaxial pullout and coupled path effect predictions)

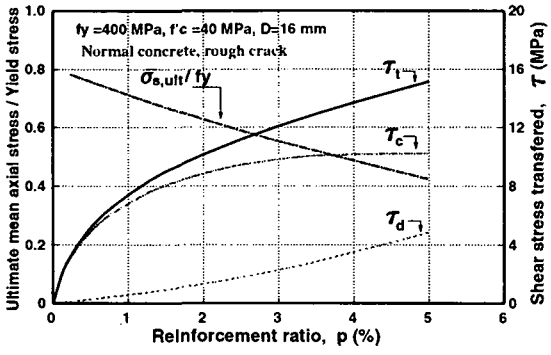

Fig.12 Variation of shear stress contributed by different mechanisms, along with reduction of axial capacity, with increasing reinforcement ratios.

stresses at a critical section inside the concrete brought about by a coupled displacement path. The damage induced in the concrete surrounding the bar further reduces this capacity due to increased transverse displacement.

However, the total capacity prediction is close to the uniaxial prediction since part of the loss of contribution to shear capacity by concrete is balanced by the shear carried by the dowel action. The uniaxial prediction cannot predict the displacement associated with the shear capacity, since true microscopic mechanism of embedded bars is not captured in such an idealization, as was discussed in the reference (15).

It is also seen that, other influencing parameters remaining the same, as the reinforcement ratio increases the mean ultimate confining axial stress in the reinforcement decreases as shown in **Fig.12**. This is also evident from test results[16]. However, the total shear transferred, τ_t, goes on increasing at a decreasing rate, which is also evident in test results conducted for this study and in literature[4),5)]. Even though the ultimate mean axial stress in the bar is lowered with the increase in p, the total confining force increases which increases the ultimate shear

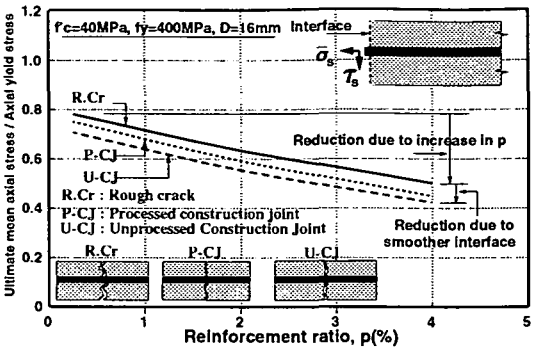

Fig.13 Reduction in ultimate mean axial stress for different surface geometry with increase in reinforcement ratio.

capacity, $\tau_{t,ult}$. This made it possible for previous researchers to find a direct empirical predictive relation between p and $\tau_{t,ult}$, although, as elaborated in this study, the actual mechanism is more complex. The contribution of concrete to shear transfer also increases with a decreasing rate but the rate of dowel contribution increases. The variation of these quantities with increasing reinforcement ratio is shown in **Fig.12**.

The sensitivity of the ultimate axial stress attained, $\overline{\sigma}_{s,ult}$ for different surface geometry, with increase in reinforcement ratio is also simulated as shown in **Fig.13**. The different geometry of crack surfaces and associated stress transfer mechanisms are taken into account in analysis with respect to different contact density functions [12] from each analysis case.

It can be seen that the sensitivity of reduction in $\overline{\sigma}_{s,ult}$ for different surface types is nearly similar. It is also clear that the reduction in $\overline{\sigma}_{s,ult}$ for increase in reinforcement ratio is greater than corresponding reduction due to smoothening of surface geometry. This is because much more rapid increase of the displacement path ratio, δ_b/S, occurs with increase in p than due to the change in the contact density function.

8. SIMULATION OF SIZE EFFECT IN RC INTERFACES

The effect of size on RC interface stress transfer behavior is an important consideration, since laboratory tests are usually limited to small scale experiments, whereas in practice considerable larger sized specimens are increasingly being used. Parametric numerical simulation was carried out to clarify the size effect, by varying bar sizes from 6 mm to 70 mm in diameter, within fixed reinforcement ratios and number of bars in the

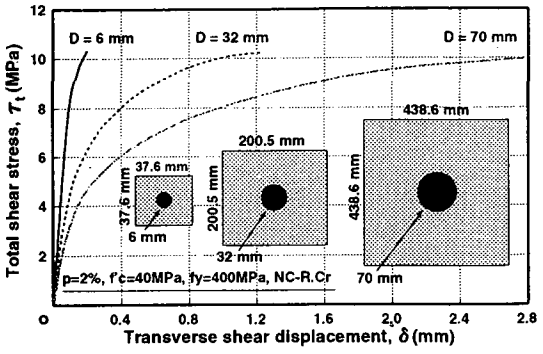

Fig.14 Shear stress versus shear displacement relationship with increase in specimen size.

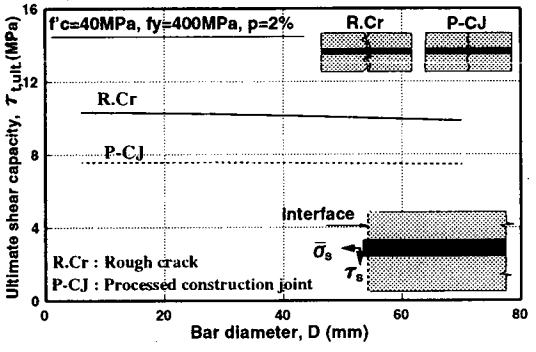

Fig.15 Ultimate shear capacity versus bar diameter relation for different surface geometry.

section. The sectional size variation thus represented an increase of 11.66 times, from the smallest to the biggest size. Concrete and steel strengths were kept constant by 40 and 400 MPa, respectively. Both rough cracks and smooth joints were analyzed.

The analytical results indicated that even though pre-peak ductility is so much affected with the increase in size, but the capacities are not so sensitive, as shown in **Fig.14**, where specimens of three different sizes with reinforcement ratio equal to 2% are illustrated. For a size increase of greater than 11 times, the drop in corresponding capacity is about 5%. The sensitivity for different surface geometry is shown in **Fig.15**, and indicates lesser variation in capacity for a smooth joint than a rough crack.

The reason for this can be understood by considering **Fig.16**, where the maximum curvature attained by different sized bars, along with the ultimate mean axial stress attained is plotted together. It can be seen that for the lower diameter bars, the maximum curvature attained is higher in comparison to bigger diameter bars, since the absolute zone size over which the curvature is distributed is small. However, the effect of curvature

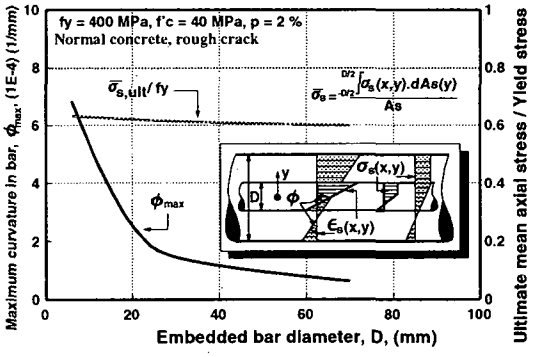

Fig.16 Relationship of maximum curvature and ultimate mean axial stress in bar versus bar diameter.

on the outer fiber strain is also lesser for a small diameter bar (theoretically speaking the effect of curvature on a bar of zero diameter is none). On the other hand, for a larger diameter bar, even though the absolute curvature is smaller, the effect on the outer fiber strain is greater. As a result, the final value of the ultimate mean axial stress attained by different diameter bars does not change much for a given reinforcement ratio.

The variation of ultimate mean axial stress with reinforcement ratio for 6 mm and 70 mm diameter bars, for different surface geometry is shown in **Fig.17** and **Fig.18**. This indicates that with the increase in reinforcement ratio, the ultimate axial stresses do vary somewhat with size, specially at higher values of reinforcement ratio, but the variation is not so sensitive. The lesser variation in smooth joints (**Fig.18**), as compared to rough cracks (**Fig.17**), can be understood by observing the relative difference between the individual curves for 6 mm and 70 mm diameter bars.

In the case of the 6 mm diameter bar, change in surface geometry brings about reduction in ultimate axial stress, but for the 70 mm diameter bar such a reduction is almost negligible. This is because the interface opening associated with the 70 mm diameter bar is relatively very high (more than 1 mm, in either case) so that changes in surface geometry does not produce any appreciable difference of ultimate mean axial bar stress at such high dilatancy. Thus the relative difference between $\overline{\sigma}_{s,ult}$ for different bar diameters is higher in rough cracks than in smooth joints, and this is the reason why size effect is relatively more pronounced in rough cracks. Since it is observed from **Fig.17** that $\overline{\sigma}_{s,ult}$ differs more with increasing reinforcement ratios, a simulation of size effect was carried out for different reinforcement ratios, as shown in **Fig.19**.

However, again it is seen from this figure that the overall capacity sensitivity to size does not increase

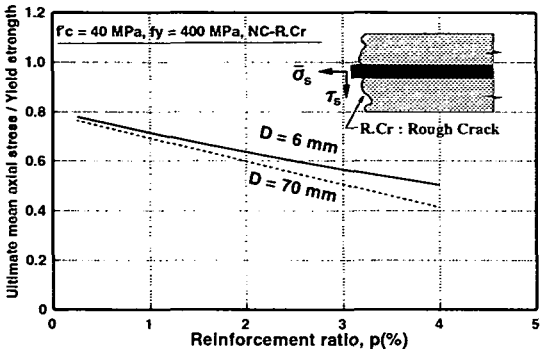

Fig.17 Relationship of ultimate mean axial stress in bar versus reinforcement ratio, for rough cracks.

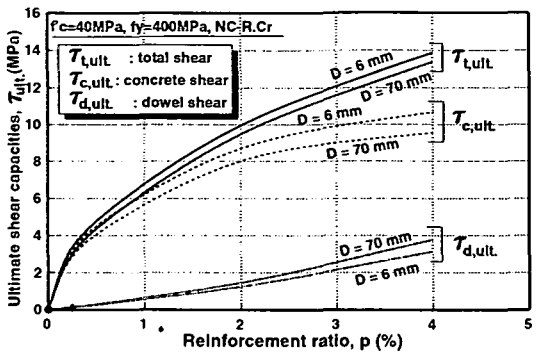

Fig.20 Relationship between ultimate shear capacity and reinforcement ratio, for different bar sizes, illustrating contribution from aggregate interlock and dowel action.

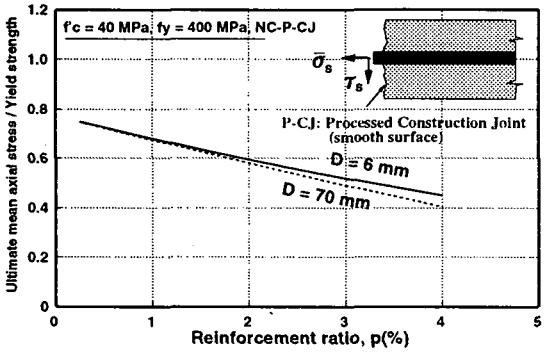

Fig.18 Relationship of mean ultimate axial stress in bar versus reinforcement ratio, for smooth joints.

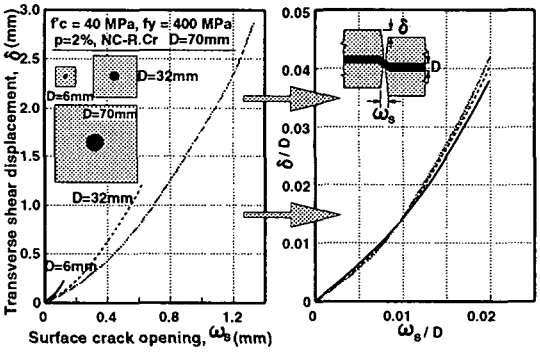

Fig.21 Relationships between absolute and normalized shear displacement and surface opening at interface, with variation in specimen size.

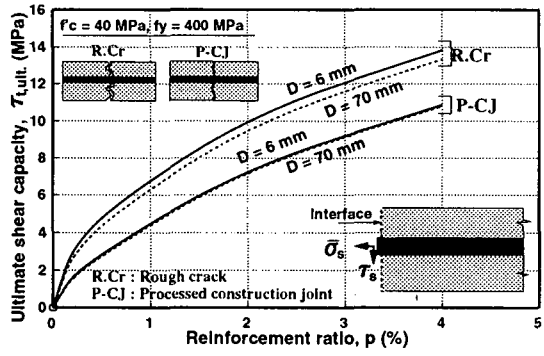

Fig.19 Relationship between ultimate shear capacity and reinforcement ratio, for different surface geometry and bar sizes.

with increasing reinforcement ratio. The reason for this can be understood by examining the components acting in the shear transfer mechanism, as shown in **Fig.20**. Although the contribution from the concrete reduces, due to lower $\overline{\sigma}_{s,ult}$ for larger diameter bars at higher reinforcement ratio, but at the same time the increased transverse displacement associated with the larger bar produces increased dowel shear, and overall the total shear capacity is not much affected.

As mentioned before that even though size effect is not substantial, the associated kinematics at the interface show significant increase in post-peak ductility with size. However, when the shear displacement, δ, and surface crack opening, ω_s, at the interface are normalized by a referential parameter for size, e.g., respective bar diameters, D, the displacement paths at the joint is uniquely defined, as shown in **Fig.21**. This indicates that there is no substantial size effect at the level of the RC interface itself under shear.

When such an interface is part of a structural member, each displacement component has its own separate effect on the member and structural level deformations. Therefore, the size effect becomes more complex and needs to be established at the member and structural levels.

Summarizing the above simulations for the size effect, it is found that shear capacity of RC interfaces is not a highly size sensitive phenomenon[4], although the associated pre-peak

ductility varies considerably with size. The primary reason for this is that the ultimate axial confining force given by the embedded bar does not vary so much with size, and the effect on total shear capacity due to the small variation that does occur at high reinforcement ratios is balanced by the correspondingly increased dowel shear. Rougher surface geometry brings about comparatively more size sensitivity. Size effect at member and structure levels need to be investigated separately due to the interface displacement.

9. CONCLUSIONS

By combining the generic bar model, under coupled axial pullout and transverse displacement slip, with an aggregate interlock model, modified by consideration of the nonlinear interaction between the reinforcement and the surrounding concrete, a unified stress transfer model to predict RC interface behavior is formulated. The formulated model brought the following conclusions.

1) Modeling of shear transferred by dowel action and aggregate interlock can be treated in a unified concept, and separate considerations and assumptions are not required for each mechanism, since generalized system of forces mobilizing each mechanism have the same origin.

2) In the case of embedded bar pushing against the concrete core, the predominant mode of interface failure is initiated by the reduction of axial stiffness of the confining reinforcement, under the coupled displacement paths to which it is subjected, and finally the complete loss of axial confinement due to the formation of a plastic hinge in the reinforcement.

3) Applicability of the proposed model is verified for the stress transfer, both normal and parallel to the crack plane, and also for the associated displacements at the interface with available test results. The accuracy of prediction of the shear capacity of rough cracks in reinforced concrete is verified from a large number of test results in literature with reinforcement normal to the shear plane.

However, the verification does not cover extremely large transverse displacement accompanying splitting cracks of cover concrete along bars and final rupture of reinforcement.

4) For reinforcement oblique to the shear plane, the proposed model can be extended to predict shear capacity by considering the increase in zone sizes for curvature and bond deterioration for cases where the bar pushes against the less confined free surface of the supporting concrete between the interface and the bar, instead of the core concrete below.

5) Displacement paths associated with shear transfer and capacity can be predicted better by utilizing rational physical concepts in the aggregate interlock model, such as reduced stress transfer arising out of the localized damage to the concrete around the bar at the interface, and the non-uniform dilatancy in concrete due to embedded bar.

6) Numerical simulations indicate that the ultimate mean axial bar stress that reduces with increase in reinforcement ratio. This verifies experimental findings. The contribution to the shear capacity from the aggregate interlock and dowel action also increases with reinforcement ratio, but at significantly different rates.

7) Simulations of size effect behavior indicates that the stress transfer behavior of RC interfaces does not exhibit pronounced size dependency, both for normal and transverse stresses. The pre-peak ductility however changes significantly with size. Structure or member level size effect, resulting from the individual kinematic component of the interface, needs to be investigated separately.

REFERENCES

1) Mackawa K., Khan, J., Qureshi, J. and Mishima, T: Reduced axial stiffness of deformed bars under shear slip along crack in concrete, *Bond in Concrete*, CEB, Latvia, pp.11-18, Oct. 1992.
2) Qureshi, J. and Maekawa K.: Computational model for steel bar embedded in concrete under combined axial pullout and transverse shear displacement, *Proc of JCI*, Vol. 15, No. 2, pp. 1249-1254, 1993.
3) Bujadham, B., Maekawa, K. and Mishima, T.: Cyclic discrete crack modeling for reinforced concrete, *Computer Aided Analysis and Design of Reinforced Concrete Structures*, Pineridge Press, pp. 1225-1236, 1990.
4) Yamada, K. and Aoyagi, Y.: Shear transfer across cracks, *Proceedings of JCI 2nd Colloquium on Shear Analysis of RC Structures*, pp.19-28, 1983.
5) Hofbeck, J. A., Ibrahim. I. O. and Mattock, A. H.: Shear transferred in reinforced concrete, *ACI Journal*, V. 66, No. 2, pp.119-128, 1969.
6) Taylor, H. P. J.: The fundamental behavior of reinforced concrete beams in bending and shear, *ACI publication SP-42*, pp.43-77, 1974.
7) Mishima, T., Yamada, K. and Maekawa, K.: Localized deformational behavior of a crack in RC plates subjected to reversed cyclic loads, *Proc. of JSCE*, No. 442/V.-16, pp.161-170, Feb., 1992.
8) Li, B., Maekawa, K. and Okamura, H.: Contact density model for stress transfer across cracks in concrete, *Journal of the Faculty of Eng.*, the University of Tokyo (B), Vol.XL, No.1, pp.9-52, March 1989.
9) Reinhardt, H. W. and Walraven, J. C.: Cracks in concrete subject to shear, *Journal of STR. Div., Proc. of the ASCE*, Vol. 108, ST1, pp.207-224, Jan. 1982.
10) Walraven, J., Frenay, J. and Pruijjsers, A: Influence of concrete strength and load history on the shear friction capacity of concrete members, *PCI Journal*, pp.66-83, Jan.-Feb., 1987.

11) Bujadham, B. and Maekawa, K.: Qualitative studies on mechanisms of stress transfer across cracks in concrete, *Proc. of JSCE*, No. 451/V-17, pp. 265-275. August 1992.
12) Bujadham, B. and Maekawa. K.: The universal model for stress transfer across cracks in concrete, *Proc. of JSCE*, No. 451/V-17, pp. 277-287. August 1992.
13) Bujadham, B., Mishima, T. and Maekawa, K.: Verification of the universal stress transfer model, *Proc. of JSCE*, No. 451/V-17, pp. 289-300, August 1992.
14) Goto, Y.: Cracks formed in concrete around deformed tension bars, *ACI Journal*, pp. 244-251. April 1971.
15) Maekawa, K. and Qureshi, J. : Computational model for reinforcing bar embedded in concrete under combined axial pullout and transverse displacement, *J. Material, Conc. Struct., Pavements., JSCE*, No.538/V-31, pp.227-239, May, 1996.
16) Maekawa, K. and Qureshi, J. : Embedded bar behavior in concrete under combined axial pullout and transverse displacement, *J. Material, Conc. Struct., Pavements., JSCE* No.532/V-30, pp.183-195, February 1996.

(Received March 27, 1996)

骨材のかみあわせとダボ作用による鉄筋コンクリート接合面の応力伝達

前川宏一・Juneid QURESHI

本研究は，面内せん断力を受ける鉄筋コンクリート接合面の一般的な挙動予測モデルを提案するものである．導出においては，ひび割れ面での応力伝達と鉄筋のダボ作用，並びに引き抜けとせん断を同時に受ける鉄筋の構成モデルが相互作用を考慮して組み合わされた．種々の指標を系統的に変化させた実験結果に基づき，提案された構成モデルの検証が行われた．